

The Seventeenth CIRP Conference on Electro Physical and Chemical Machining (ISEM)

Ultrasonic assisted creep feed grinding of Inconel 718

D. Bhaduri^a, S.L. Soo^{a,*}, D. Novovic^b, D.K. Aspinwall^a, P. Harden^c, C. Waterhouse^d,
S. Bohr^e, A.C. Mathieson^f, M. Lucas^f

^a*Machining Research Group, School of Mechanical Engineering, University of Birmingham, Edgbaston, Birmingham, B15 2TT, UK*

^b*Turbines, Rolls-Royce plc, Derby, DE24 9BD, UK*

^c*Element Six Ltd., Shannon, Co. Clare, Republic of Ireland*

^d*Hardinge Machine Tools, Whetstone, Leicester, LE8 6BD, UK*

^e*Saint-Gobain Diamantwerkzeuge GmbH & Co. KG, Schützenwall 13-17, D-22844 Norderstedt, Germany*

^f*Systems, Power & Energy Division, School of Engineering, University of Glasgow, Glasgow, G12 8QQ, UK*

* Corresponding author. Tel.: +44-121-414-4196; fax: +44-121-414-4201. E-mail address: s.l.soo@bham.ac.uk.

Abstract

The paper details the effects of depth of cut and vibration amplitude when ultrasonic assisted (US) creep feed grinding Inconel 718 with an open structured alumina based wheel. The workpiece was actuated at a constant frequency (~20.5kHz) via a block sonotrode attached to a 1kW piezoelectric transducer-generator system. A full factorial experimental array comprising 12 tests was conducted involving variation in depth of cut (0.1, 0.5 and 1.0mm), amplitude of vibration (high and low) and grinding condition (with and without vibration). Wheel speed and table feed were fixed at 30m/s and 600mm/min respectively for all tests. Application of ultrasonic vibration resulted in reductions in vertical (F_v) and horizontal (F_h) force components by up to 28% and 37% respectively, however greater wheel wear (30-60% lower G-ratio) occurred under hybrid operation due to increased grit/bond fracture. SEM micrographs of the slots machined with US assistance revealed higher levels of side flow/ploughing in comparison to standard creep feed ground specimens. Additionally, more overlapping grit marks were visible on surfaces subject to ultrasonic assisted grinding. Increasing amplitude of vibration produced lower grinding forces (up to 30% for F_v and 43% for F_h) but higher workpiece surface roughness (up to 24%). Topographic maps of grinding wheel surface replicas indicated that use of US vibration generally led to an increase in the number of active cutting points on the wheel.

© 2013 The Authors. Published by Elsevier B.V. Open access under [CC BY-NC-ND license](https://creativecommons.org/licenses/by-nc-nd/4.0/).

Selection and/or peer-review under responsibility of Professor Bert Lauwers

Keywords: Grinding; nickel; ultrasonics; vibration.

1. Introduction

Nickel based superalloys are used extensively in the hotter sections of gas turbine engines, as they are able to maintain their strength and corrosion resistance (at temperatures above ~700°C) better than other metallic alloys. As a result of continuous development over the last ~60 years, the range of superalloys in use is far more comprehensive than generally appreciated [1], however a common feature is their relatively poor machinability as detailed by a number of researchers [2-3]. Despite recent gains in abrasive machining performance/productivity through the development and use of more open structured wheel systems/grit

morphologies and greater emphasis on high pressure fluid use as typified by the ‘VIPER grinding’ approach utilising conventional abrasives [4], the efficient grinding of aeroengine components remains a challenge, particularly when viewed against anticipated product/market growth [5].

Hybrid approaches to machining whereby two or more complementary cutting techniques are used simultaneously to achieve greater productivity or enhance product quality, are well documented but not extensively used by industry [6-7]. Ultrasonic or vibration assisted grinding (UAG) falls under this heading and reference to this can be found in early work by Colwell [8] undertaken in the 1950’s. More recently, Nakagawa et al. [9] observed that when grinding

ceramic materials with ultrasonic assistance, larger depths of cut were achievable leading to higher material removal rates (MRR) and improved dimensional accuracy, together with a 60-70% reduction in normal grinding force. The majority of published papers on UAG report significant reductions in normal and tangential grinding forces (~30-50%) [10-12], together with a reduction in thermal damage/grinding burn and improvement in workpiece surface finish [10-14]. Several papers however, have reported an increase in workpiece R_a due to increased wheel wear [15].

To date, research on UAG has focussed mainly on the surface grinding of materials such as ceramics and glass together with various grades of steel. Information relating to advanced aerospace materials is extremely limited [16]. Additionally the majority of published work over the past ~20 years has largely involved vibration applied to the workpiece as opposed to the grinding wheel, primarily due to the comparatively simpler experimental setup. This approach has been adopted in the present research involving the creep feed grinding of Inconel 718 workpieces with an open structured alumina wheel. The objective of the work was to investigate the effects of depth of cut (a_e) and amplitude of US vibration on grinding forces (vertical and horizontal), wheel wear (G-ratio), workpiece surface roughness/quality (2D and 3D parameters) as well as wheel surface topography.

2. Experimental details

The experimental trials were conducted on a Bridgeport FGC1000 flexible grinding centre, with a maximum spindle speed of 6000rpm and power rating of 25kW. Rectangular blocks of solution treated and aged Inconel 718 (hardness of $\sim 44 \pm 1$ HRC) measuring 110x55x7mm were used as the workpiece material. These were clamped onto a specially designed aluminium table/block sonotrode mounted on the machine worktable, which was connected to a 1kW piezoelectric transducer-generator system. The transducer was attached to transmit the US vibration in a direction parallel to grinding feed. The alumina grinding wheels known commercially as POROS2 had a plain geometry, vitrified bond, open structure, a diameter of 220mm and a width of 25mm.

The full factorial experimental array comprised 12 tests involving variations in depth of cut (0.1, 0.5 and 1.0mm), amplitude of vibration (high and low) and grinding condition (with and without vibration). No replications were performed due to the limited availability of workpiece material. Wheel speed and table feed were fixed at 30m/s and 600mm/min with all trials performed in a down grinding creep feed mode without spark-out. The experimental array is shown in

Table 1. Each test involved a single grinding pass on the workpiece (55mm cut length).

Table 1. Full factorial experimental array

Test no.	Depth of cut, a_e (mm)	Amplitude of vibration	Vibration
1	0.1	0	OFF
2	0.1	High	ON
3	0.1	0	OFF
4	0.1	Low	ON
5	0.5	0	OFF
6	0.5	High	ON
7	0.5	0	OFF
8	0.5	Low	ON
9	1.0	0	OFF
10	1.0	High	ON
11	1.0	0	OFF
12	1.0	Low	ON

Dressing of the POROS2 wheel (after each trial) was carried out using a diamond roller dresser (Φ 105mm) with an average grain size of $\sim 800\mu\text{m}$ and spacing of $\sim 1.5\text{mm}$. Two high pressure pumping systems were used to supply fluid for wheel cleaning (70bar) and into the grinding zone (30bar) via laminar flow nozzles. The grinding fluid was a water-based synthetic oil product, Trim C270, with a concentration of 7–10%.

For trials involving US vibration, the workpiece was actuated at a constant frequency of $\sim 20.5\text{kHz}$, while the amplitude of vibration was specified on the generator in terms of a percentage scale ranging from 0 to 100%. The actual amplitude of the block sonotrode under zero-load condition and vibrating at the 70% setting was measured using a YP0901B ultrasonic amplitude-meter (Hangzhou Success Ultrasonic Equipment Co. Ltd.) having a sensitivity of $1\mu\text{m}$; together with a Polytech OFV 3001 Laser Doppler Vibrometer coupled to an OFV 303 sensor head, see Figure 1 for x-axis measurement arrangement.

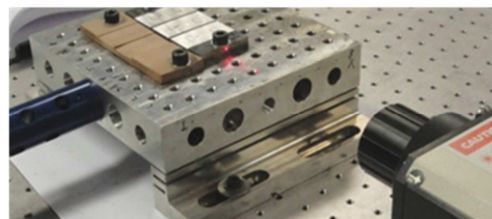


Fig. 1. Measurement of x-axis amplitude with laser vibrometer

Two different settings of the ultrasonic generator were used in order to generate two levels of amplitude of vibration, hereafter termed as 'High' and 'Low'. The maximum amplitudes recorded at 'High' and 'Low' settings were $\sim 7\text{-}8\ \mu\text{m}$ and $2\text{-}4\ \mu\text{m}$ respectively. The

experimental setup for measuring the amplitude of vibration of the block sonotrode using a mechanical amplitude-meter is shown in Fig. 2(a) while the on-machine configuration of the wheel-workpiece-sonotrode arrangement is detailed in Fig. 2(b).

Vertical (perpendicular to feed direction) and horizontal (parallel to feed direction) grinding forces were measured using a Kistler 9257A 3-component piezoelectric dynamometer coupled to charge amplifiers and a PC running Dynaware software. In order to determine the G-ratio, wheel diameters were measured before and after each grinding trial using a DEA Swift manual coordinate measuring machine (CMM) connected to a computer programmed with Delcam Power Inspect software. The wheels were assessed at 30 different points around the periphery, each at 5 different levels of the wheel width.

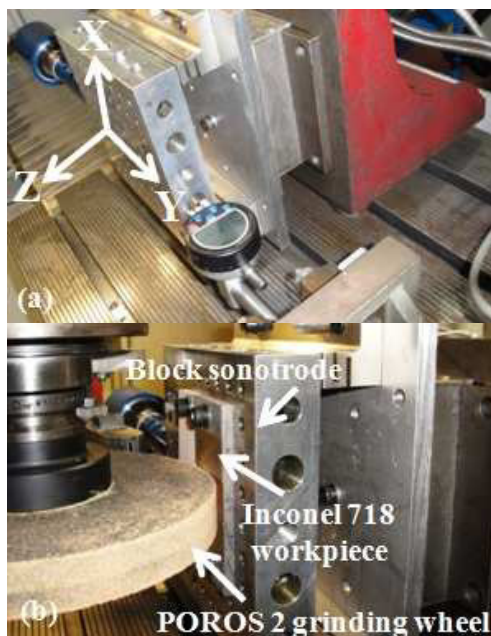


Fig. 2. Experimental setup; (a) measurement of amplitude of vibration of the block sonotrode using a mechanical amplitude-meter, (b) on-machine configuration of wheel-workpiece-sonotrode arrangement

Both 2D and 3D topographical profiles of the ground workpiece surfaces were recorded using a Taylor Hobson Form Talysurf 120L, with 2D assessment involving a 0.8mm cut-off (average of 3 measurements). Micrographs of the ground surfaces were taken using a JEOL 6060 scanning electron microscope (SEM). Due to space restrictions in the SEM chamber, wheel surface topography was assessed by producing negative and positive replicas using a graphite block and rubber-resin compound respectively. For the former, the worn wheel was used to grind a graphite block at a wheel speed of 15m/s, table speed of 150mm/min and depth of cut of 1.0mm. The resulting surface profiles were then traced,

which represented negative profiles of the wheel surface (assumed zero wear from grinding of graphite block). In contrast, positive replicas of the wheel surfaces were obtained using a synthetic rubber and resin replicating compound (Microset), after which 3D surface profiles were measured using the Form Talysurf system. Statistical analysis (analysis of variance - ANOVA) on the recorded data was performed using Minitab software.

3. Results and discussion

3.1. Grinding forces, radial wheel wear and G-ratio

Figure 3 shows the vertical (F_v) and horizontal (F_h) grinding forces both with and without US vibration. A rise in vertical grinding forces (F_v) was observed when depth of cut increased from 0.1mm to 1.0mm. This was due to an increase in the undeformed chip thickness as well as chip length. No such trend was apparent when horizontal grinding forces (F_h) were considered. The majority of tests showed lowering of both vertical (F_v) and horizontal (F_h) grinding forces by up to 28% and 37% respectively, when grinding was employed with vibration. As outlined in the literature, this was probably due to a reduction of thermal load on the abrasive grits, caused by intermittent cutting action of the grains under ultrasonic actuation [16]. The anticipated lower temperatures most likely resulted in decreased localised welding/adhesion between the high asperities of the work surfaces, grits and loaded material within pores of the wheel [17], thereby lowering frictional forces. Ultrasonic operation with the 'Low' amplitude setting rendered higher grinding forces than those obtained with 'High' amplitude of vibration. The engagement of more active grits during cutting with the lower vibration amplitude is a possible reason, as evident from SEM micrographs of the wheel replicas shown in Section 3.3.

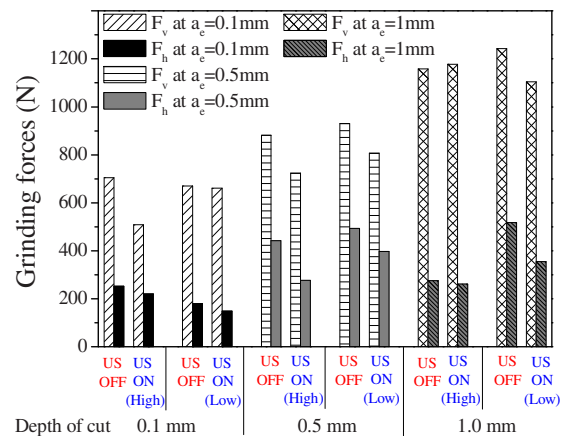


Fig. 3. Vertical (F_v) and horizontal (F_h) grinding forces under different grinding conditions

Table 2 gives the percentage contribution ratios of different response measures for different factors and interactions as obtained from ANOVA. Depth of cut was observed to have a significant effect on both components of grinding force (91.1% and 54.9% for F_v and F_h respectively).

Table 2. Percentage contribution ratios of factors obtained from ANOVA

Factors	Percentage contribution ratios (PCR's)					
	F_v	F_h	G-ratio	W/P R_a	W/P S_a	Graphite S_a
Depth of cut (a_c)	91.1*	54.9*	55.8*	22.1	20.8*	57.7*
Amplitude (Amp)	1.4	13.3	1.4	25.0*	55.2*	28.9*
Vibration (Vib)	4.8*	12.8	22.2*	0.4	6.2	4.7*
$a_c \times \text{Amp}$	0.6	8.6	1.9	10.8	3.9	1.0
$a_c \times \text{Vib}$	0.5	2.9	8.4	6.3	9.4	0.3
$\text{Amp} \times \text{Vib}$	0.0	2.7	3.7	21.1	0.7	1.3
$a_c \times \text{Amp} \times \text{Vib}$	1.6	4.8	6.6	14.3	3.8	6.1

* Statistically significant factors at the 5% level

The effects of depth of cut and amplitude of vibration on radial wheel wear (Δr_s) and G-ratio are shown in Fig 4. Wheel wear was found to be almost negligible (2-3 μm) at a depth of cut of 0.1mm when grinding was carried out without vibration. In general, radial wheel wear increased as depth of cut was varied from 0.1 to 1.0mm. However, the main effects plot of wheel G-ratio (graph not shown) similarly showed an increase with a rise in depth of cut from 0.1mm to 1.0mm, due to a greater percentage rise in volume of material removed than that of radial wheel wear.

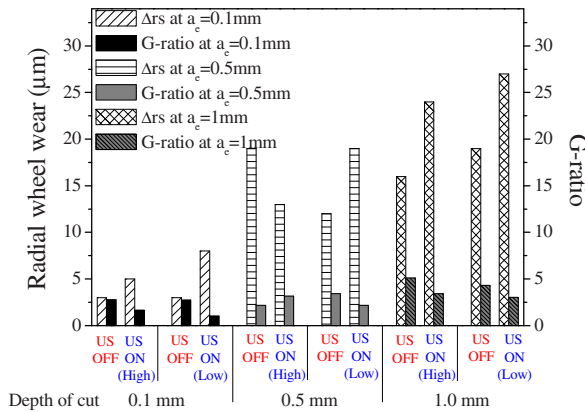


Fig. 4. Radial wheel wear and G-ratio under different conditions

When ultrasonic actuation was employed, wheel G-ratio reduced by 30-60% in 5 out of 6 tests. The radial component (in the Z-direction) of ultrasonic vibration imparted a higher mechanical load on the grits together with a load-relieving phase [16]. This led to micro-

splintering of the alumina grits as well as fracture of the associated bond, resulting in higher wheel wear with the hybrid configuration. Main effects plot showed that the 'Low' amplitude setting rendered marginally lower G-ratio than that obtained with the 'High' amplitude level; however this factor was not statistically significant according to ANOVA calculations.

3.2. Workpiece surface topography and quality

Figures 5 and 6 depict 2D surface roughness (R_a) and 3D topographical parameters (S_a , S_t , S_z) respectively. Values of R_a of the ground surfaces generally decreased from the start to the end of cut due to generation of wear flats on the grits as grinding progressed. However, no significant variation in R_a was observed with change in depth of cut from 0.1 to 1.0mm.

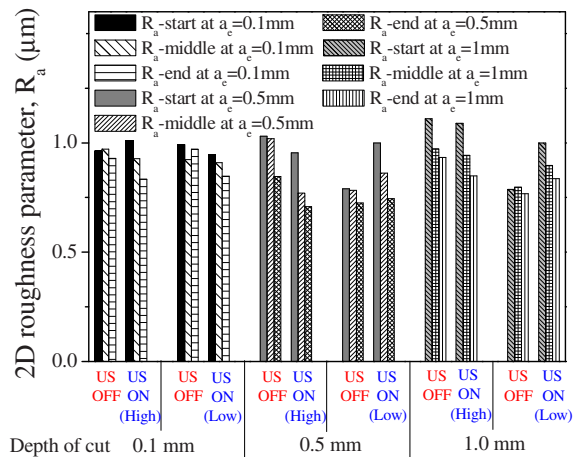


Fig. 5. 2D surface roughness (R_a) of ground workpiece surfaces

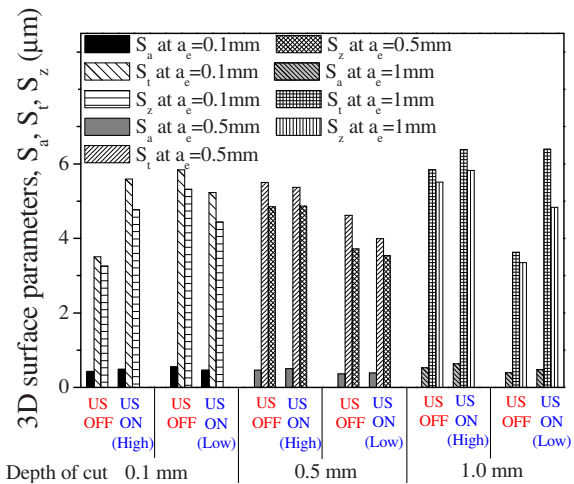


Fig. 6. 3D topographical parameters of ground workpiece surfaces

Both R_a and S_a of the ground workpieces generally increased with the assistance of US vibration in

comparison to those obtained without vibration. This was possibly the result of increased smearing and side flow/ploughing of the workpiece material when operating with vibration (seen from the SEM micrographs in Fig. 7(c) and 7(d)), which was caused by lateral movement of the grits under multi-modal ultrasonic actuation [11]. The data also suggests greater plastic deformation [15] of the workpiece material due to the higher mechanical loading imparted from the application of vibration [16]. In contrast, some pull-out of the material was observed when grinding was employed without vibration (Fig. 7(b)), which was absent on the surfaces subject to US actuation.

The majority of tests also showed that the maximum depth of valley S_v of the ground surfaces was generally higher in the hybrid mode in comparison to those obtained in conventional CFG (not shown in graph). This was thought to be due to the action of vibration along the Z-axis of the block sonotrode, i.e. in a direction radial/normal to the wheel surface. The main effects plot relating to workpiece surface roughness showed that the vibration setting with ‘High’ amplitude resulted in higher R_a and S_a in comparison to those obtained with the ‘Low’ amplitude setting, suggesting that the latter led to greater numbers of active cutting points/grits in contact with the work surface. This also explains the reason for higher grinding forces obtained with the latter setting in comparison to those obtained with the former. The ANOVA showed that variation in amplitude of vibration (High and Low) had a significant effect on the R_a and S_a of ground workpiece surfaces (25% and 55.2% respectively), see Table 2.

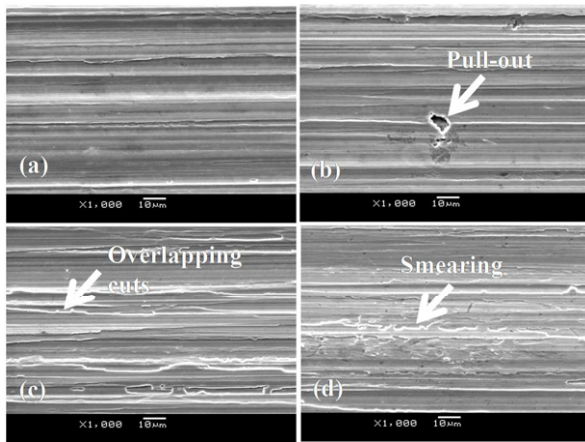


Fig. 7. SEM micrographs of representative ground workpiece surfaces machined; (a) & (b) without vibration, (c) & (d) with vibration

3.3. Grinding wheel surface evaluation

The average surface roughness (S_a) of the graphite blocks and density of peaks (S_{ds}) from the resin replicas

are shown in Fig. 8. The S_{ds} parameter provides an indication of the static cutting edge density [18]. The SEM micrographs of the resin replicas obtained at different amplitude settings and at a depth of cut of 1.0mm are shown in Fig. 9. Both the R_a (not shown in graph) and S_a values of the graphite replicas were generally lower when grinding was performed with US vibration in comparison to plain grinding, which suggests greater uniformity of the resulting grit heights. This was most likely caused by the ‘conditioning effect’ of the vibration. The ‘Low’ amplitude vibration setting resulted in lower R_a and S_a values of the graphite replicas in comparison to those obtained with the ‘High’ amplitude setting.

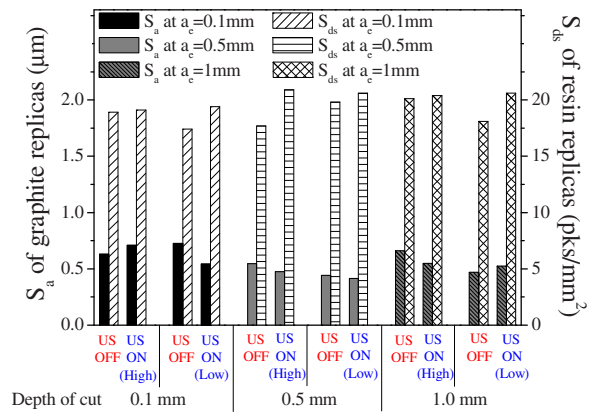


Fig. 8. S_a of graphite and S_{ds} of resin replicas of the wheel surface

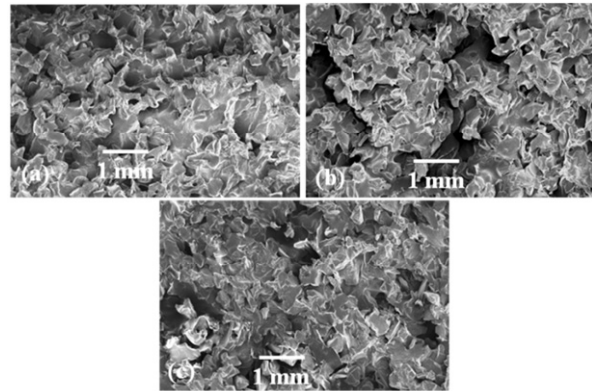


Fig. 9. SEM micrographs of representative wheel surface resin replicas following grinding; (a) without vibration (b) with vibration at ‘High’ amplitude, (c) with vibration at ‘Low’ amplitude

Statistical analysis showed that depth of cut had the highest percentage contribution on R_a and S_a of graphite replicas (50.9 and 57.7% respectively) followed by amplitude of vibration (18.3 and 28.9% respectively). Both factors had a significant effect on the S_a of graphite replicas as obtained from the F-test (Table 2).

The density of peaks (S_{ds}) of the resin (positive) replicas was found to increase in all trials where vibration was applied. This was attributed to the greater number of active cutting points per grain (due to grit fracture) generated with use of US vibration. Butler et al. [19] suggested that a decrease in S_{ds} value signalled loss of grain sharpness.

The SEM micrographs of resin replicas subject to US vibration showed that more voids/pores were generated in between grains; see Fig. 9(b) and 9(c), compared to conventional CFG (Fig. 9(a)); suggesting more grit/bond fracture due to vibration. This could be a possible reason for the lower G-ratio values measured under hybrid operation. Furthermore, larger voids/pores were observed on the wheel surface following grinding involving the 'High' amplitude setting (Fig. 9(b)), which corresponded with lower grinding forces but higher workpiece surface roughness as opposed to those obtained with the 'Low' amplitude setting.

4. Conclusions

- The application of ultrasonic vibration resulted in reductions in vertical (F_v) and horizontal (F_h) grinding forces by up to 28% and 37% respectively, however greater wheel wear (30-60% lower G-ratio) occurred under hybrid operation due to increased grit/bond fracture.
- An increase in amplitude of vibration produced lower grinding forces (up to 30% for F_v and 43% for F_h) but higher workpiece surface roughness (up to 24%).
- SEM micrographs of ground workpiece surfaces revealed greater side flow/ploughing when employing vibration assistance in comparison to standard creep feed ground specimens. Additionally, more overlapping grit marks were visible on surfaces produced with ultrasonic assisted grinding.
- Three-dimensional topographic measurement of grinding wheel surface replicas indicated that US vibration led to an increase in the number of active cutting points on the wheel. A higher amplitude of vibration rendered more voids/pores on the wheel surface, which resulted in lower grinding forces but higher surface roughness in comparison to those obtained when grinding was carried out with low amplitude of vibration.

Acknowledgements

We gratefully acknowledge the help and support from the University of Glasgow for facilities to measure the vibrational amplitude of the block sonotrode. We are also indebted to Mr. M. Prokic of MP Interconsulting for

technical advice on the ultrasonic transducer/generator system. Thanks are also due to Rolls-Royce, Element Six, Saint-Gobain Abrasives and Hardinge Machine Tools for funding, tooling and technical support.

References

- [1] Reed, R.C., 2006. *The Superalloys: Fundamentals and Applications*. Cambridge University Press, New York. ISBN-13 978-0-521-85904-2.
- [2] Jawahir, I.S., Brinksmeier, E., M'Saoubi, R., Aspinwall, D.K., Outeiro, J.C., Meyer, D., Umbrello, D., Jayal, A.D., 2011. Surface integrity in material removal processes: Recent advances. *CIRP Annals – Manufacturing Technology* 60/2, p. 603-626.
- [3] Yao, C.F., Jin, Q.C., Huang, X.C., Wu, D.X., Ren, J.X., Zhang, D.H., 2012. Research on surface integrity of grinding Inconel 718. *International Journal of Advanced Manufacturing Technology*, DOI 10.1007/s00170-012-4236-7.
- [4] Hitchiner, M., 2007. "Grinding in the aerospace industry," *Advances in Abrasive Technology X*, ISAAT. Michigan, USA, p. 491-497.
- [5] Kappmeyer, G., Hubig, C., Hardy, M., Witty, M., Busch, M., 2012. Modern machining of advanced aerospace alloys - Enabler for quality and performance. *Procedia CIRP* 1, p. 28-43.
- [6] Kozak, J., Rajurkar, K.P., 2000. "Hybrid machining process evaluation and development," *Proceedings of the 2nd International Conference on Machining and Measurements of Sculptured Surfaces*. Krakow, Poland, p. 501-536.
- [7] Lauwers, B., 2011. Surface integrity in hybrid machining processes. *Procedia Engineering* 19, p. 241-251.
- [8] Colwell, L.V., 1956. The effects of high-frequency vibrations in grinding. *Transactions of ASME* 78, p. 837-845.
- [9] Nakagawa, T., Suzuki, K., Uematsu, T., Kimura, M., Yoshida Kogyo, K.K., 1998. Development of a new turning centre for grinding ceramic materials. *Annals of CIRP* 37, p. 319-322.
- [10] Tawakoli, T., Azarhoushang, B., 2008. Influence of ultrasonic vibrations on dry grinding of soft steel. *International Journal of Machine Tools & Manufacture* 48, p. 1585-1591.
- [11] Tawakoli, T., Azarhoushang, B., Rabiey, M., 2009. Ultrasonic assisted grinding of soft steel. *Industrial Diamond Review* 1, p. 40-44.
- [12] Tawakoli, T., Azarhoushang, B., Rabiey, M., 2009. Ultrasonic assisted dry grinding of 42CrMo4. *International Journal of Advanced Manufacturing Technology* 42, p. 883-891.
- [13] Yan, Y., Zhao, B., Liu, J., 2009. Ultraprecision surface finishing of nano-ZrO₂ ceramics using two-dimensional ultrasonic assisted grinding. *International Journal of Advanced Manufacturing Technology* 43, p. 462-467.
- [14] Gao, G.F., Zhao, B., Xiang, D.H., Kong, Q.H., 2009. Research on the surface characteristics in ultrasonic grinding nano-zirconia ceramics. *Journal of Materials Processing Technology* 209, p. 32-37.
- [15] Spur, G., Holl, S.E., 1996. Ultrasonic assisted grinding of ceramics. *Journal of Materials Processing Technology* 62, p. 287-293.
- [16] Uhlmann, E., 1998. Surface formation in creep feed grinding of advanced ceramics with and without ultrasonic assistance. *Annals of CIRP* 47, p. 249-252.
- [17] Yossifon, S., Rubenstein C., 1982. Wheel wear when grinding workpieces exhibiting high adhesion. *International Journal of Machine Tool Design and Research* 22, p. 159-176.
- [18] Blunt, L., Ebdon, S., 1996. The application of three-dimensional surface measurement techniques to characterizing grinding wheel topography. *International Journal of Machine Tools & Manufacture* 36, p. 1207-1226.
- [19] Butler, D.L., Blunt, L.A., See, B.K., Webster, J.A., Stout, K.J., 2002. The characterisation of grinding wheels using 3D surface measurement techniques. *Journal of Materials Processing Technology* 127, p. 234-237.